USAFETAC/TN--92/005

CLIMATOLOGICAL PROBABILITY
of
CLOUD-FREE LINE-OF-SIGHT

by

Captain Anthony J. Warren

DECEMBER 1992

APPROVED FOR PUBLIC RELEASE;
DISTRIBUTION IS UNLIMITED.

USAF
ENVIRONMENTAL TECHNICAL
APPLICATIONS CENTER

Scott Air Force Base, Illinois, 62225-5116

REVIEW AND APPROVAL STATEMENT

USAFETAC/TN--92/005, *Climatological Probability of Cloud-Free Line-of-Sight,* December 1992, has been reviewed and is approved for public release. There is no objection to unlimited distribution of this document to the public at large, or by the Defense Technical Information Center (DTIC) to the National Technical Information Service (NTIS).

Walter F. Miller

WALTER F. MILLER, Maj, USAF
Chief, Simulations and Techniques Branch

FOR THE COMMANDER

Walter S. Burgmann

WALTER S. BURGMANN
Scientific and Technical Information
Program Manager
28 December 1992

REPORT DOCUMENTATION PAGE

2. Report Date: December 1992

3. Report Type: Technical Note

4. Title: Climatological Probability of Cloud-Free Line-of-Sight

6. Author: Capt Anthony J. Warren

7. Performing Organization Names and Address: United States Air Force Environmental Technical Applications Center (SYT), Scott AFB, IL 62225-5116

8. Performing Organization Report Number: USAFETAC/TN--92/005

12. Distribution/Availability Statement: Approved for public release; distribution is unlimited.

13. Abstract: This report describes how the climatological frequency distribution of cloud-cover is obtained and used to compute the climatological probability of cloud-free line-of-sight, or CFLOS. The probabilities can be estimated for an instantaneous point in time or for a specified time window (i.e., the probability of a continuous CFLOS for a time period of t minutes). The procedures outlined in the report are used by the USAF Environmental Technical Applications Center (USAFETAC) CPCFLOS computer program. An appendix describes the Burger Aerial Algorithm.

14. Subject Terms: CLIMATOLOGY, WEATHER, METEOROLOGY, CLOUDS, CLOUD COVER, SKY COVER, EARTH COVER, OBSERVATIONS, ANALYSIS, CLOUD ANALYSIS, NEPHANALYSIS, LINE-OF-SIGHT, CLOUD-FREE LINE-OF-SIGHT, PROBABILITIES, STATISTICS, COMPUTER PROGRAMS, ALGORITHMS, BURGER AERIAL ALGORITHM,

15. Number of Pages: 31

17. Security Classification of Report: Unclassified

18. Security Classification of this Page: Unclassified

19. Security Classification of Abstract: Unclassified

20. Limitation of Abstract: UL

Standard Form 298

PREFACE

The Climatological Probability of Cloud-Free Line-of-Sight (CPCFLOS) program was developed by the United States Air Force Environmental Technical Applications Center's Environmental Simulation and Techniques Branch (USAFETAC/SYT) to meet the many requests for cloud-free line-of-sight (CFLOS) statistics needed in the testing and deployment of various Department of Defense optical sensing systems. The CPCFLOS program merged existing capabilities of several programs (ECS3DCFL and DNYCPCF) into one and corrected some inconsistenceies found in these individual programs under project number 7081503.

The purpose of this technical note is to describe the methodologies and algorithms used to generate climatological probabilities of CFLOS. The CPCFLOS software employs three main algorithms: the Burger Aerial Algorithm to enhance the fidelity of observed cloud cover, the SRI model to relate fractional sky cover to CPCFLOS, and the Keilson-Ross Algorithm to estimate the duration probabilities of CFLOS.

TABLE OF CONTENTS

FIGURES

TABLES

1. INTRODUCTION

The United States Air Force Environmental Technical Applications Center (USAFETAC) is frequently tasked to provide statistics on the probability of cloud-free line-of-sight (CFLOS) for the design and testing of the optical components of various Department of Defense systems. The *climatological probability of CFLOS* is the percentage of time a cloud-free line-of-sight occurs at a particular location as a function of month, time-of-day, and viewing angle. However, conventional weather observations only contain data on cloud cover, not on the distribution of clouds in the sky dome. As a result, a simulation model is required to relate cloud cover climatology to statistics on the climatological probability of CFLOS. CFLOS calculations can be required for a wide variety of viewing configurations. This report is limited to one class of viewing: a line-of-sight that runs from a point on the earth's surface to a point in space. (For discussions of other types of viewing see Harms, 1986; Warren, 1991*a*; Rupp and Warren, 1992).

At USAFETAC, cloud climatologies are derived from two main sources. The first is the USAFETAC surface database, which is a worldwide collection of surface weather observations. The second data source is the Air Weather Service Real Time Nephanalysis (RTNEPH). This is a worldwide cloud analysis derived from surface and satellite cloud cover analyses (Kiess and Cox, 1988). From either of these sources, the frequency distribution of total cloud-cover can be computed. This report describes how the climatological frequency distribution of cloud-cover is obtained and used to compute the climatological probability of CFLOS. The probabilities can be estimated for an instantaneous point in time or for a specified time window (i.e., the probability of a continuous CFLOS for a time period of *t* minutes). The procedures outlined in the report are used by the USAFETAC computer program CPCFLOS.

2. CLOUD-COVER FREQUENCY DISTRIBUTION

2.1 Introduction. The climatological probability of cloud-free line-of-sight (CPCFLOS) is derived from the climatological cloud-cover frequency distribution. These distributions can be obtained from surface observations, satellite analyses, or a combination of these two sources. None of these is an *ideal* data source. S·.rface observations suffer several problems; e.g., observer bias, poor resolution of reporting codes, and differences in local reporting practices. Satellite analyses have documented deficiencies as well. (For a review of some of the biases in the RTNEPH total cloud-cover analysis, see Lowther *et al.*, 1991). More fundamentally, surface and satellite observations of total cloud-cover are actually two different physical phenomena (Snow, 1990). This point is illustrated in Figure 1. Although no correction is made for this fact with the RTNEPH, substantial errors can result in estimating CPCFLOS if it is not taken into account.

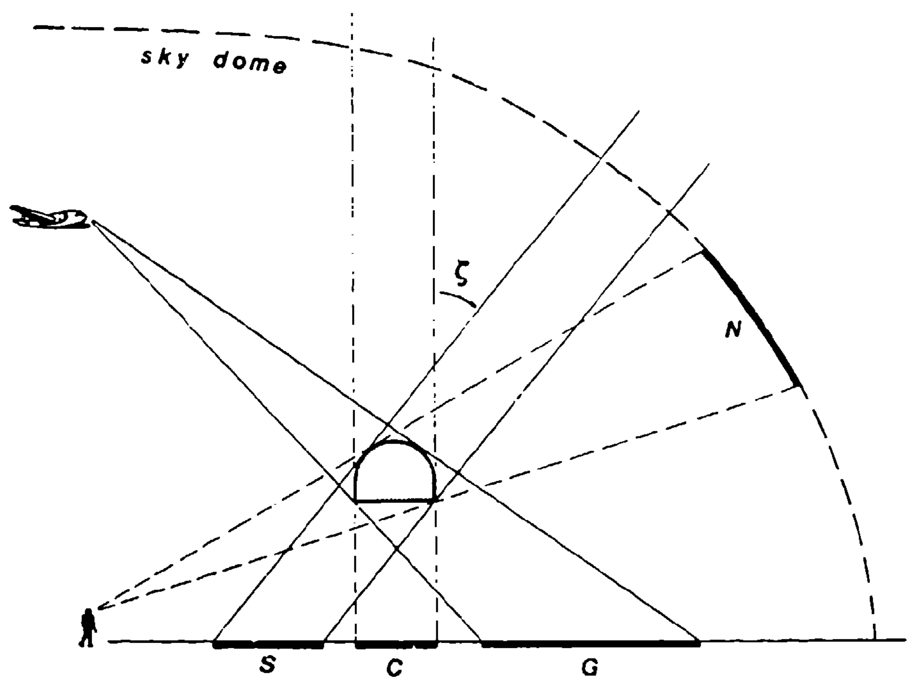

Figure 1. Viewing perspectives of total cloud-cover. S- apparent cloud cover, C- cloud cover, G - ground cover, N - sky cover. ζ is the view angle (from Snow, 1990).

These problems must be all taken into account to properly compute CPCFLOS probabilities. As a result, the computation of the cloud-cover frequency distribution is not as straightforward as merely binning cloud-cover reports over a given period of record. A statistical technique must be used to convert the low fidelity cloud-cover reports to a higher fidelity distribution. Separate binning must be made of surface-based and satellite-based cloud-cover reports. This is very important when processing RTNEPH cloud-cover reports since the RTNEPH is a blend of these two sources of data. At some locations, the climatology will be nearly entirely surface or satellite-based; at other locations it will be a mixture of these two sources.

2.2 Surface Reports of Total Cloud Cover. Surface observations are reported with either the Airways, METAR, or synoptic code. Each of these codes uses a different encoding procedure to report the observations.

2.2.1 Airways Code. With the Airways code, the observer reports cloud cover as one of four categories: clear (CLR), scattered (SCT), broken (BKN), or overcast (OVC). The observer reports the total cloud cover and base of each layer of cloud, beginning with the lowest layer. The reported total cloud cover reported is cumulative. Thus the category reported for the last layer (the layer with the highest observed base), is also the *total* cloud-cover. Unfortunately, there is not a common standard definition of these four categories. Table 1 compares the Air Force/Navy and National Weather Service/Federal Aviation Administration definitions of these categories (FMH-1, 1988). In addition to these four cloud-cover categories, two other classes may be reported: *partially obscured* and *totally obscured.* An obscuration is a surface-based visual obstruction to the cloud layer (fog, haze, and snow are probably the most frequently occurring obscurants). A *total* obscuration means that the entire sky dome is obstructed. If any portion of a cloud-layer or the clear sky is visible, then the obstruction is *partial.* The observer then carries a report in the remarks section of the observation stating the fraction (in tenths) of the sky dome that is obscured and the nature of the obscurant (e.g., the remark "F8" means that fog obscures 8/10 of the sky dome). Cloud distributions for airways reporting stations are initially obtained by computing the relative frequency of each of the four cloud classes. Generally, only a small percentage of observations are reported as either totally obscured or partially obscured. Totally obscured conditions can be binned with the OVC category. Partial obscuration of the sky dome can be as small as one-tenth or as large as nine-tenths. We have arbitrarily selected to bin these partial obscurations as BKN. However, the fraction of observations reporting a partial obscuration is small, and this assumption will have little (if any) effect on the subsequent frequency distribution.

TABLE 1. Comparison of the definitions of the Airways cloud-cover categories as used in the United States (FMH-1, 1988).

Category	National Weather Service/ Federal Aviation Administration	Air Force/Navy
CLR	Cloudless or sky-cover less than 1/10. (round to the nearest tenth)	Cloudless.
SCT	Sky-cover between 1/10 and 5/10 inclusive.	Sky-cover between a trace and 5/10, inclusive.
BKN	6/10 through 9/10, inclusive.	Greater than or equal to 6/10, but not completely overcast.
OVC	Greater than 9/10, or completely overcast.	Completely overcast.

2.2.2 Synoptic Code. The synoptic code has a field reserved for reporting the total cloud-cover in eighths (a single number between 0 and 8 is used). As with the Airways code, two additional values are used for obscured conditions: 9 for partially obscured and 10 for totally obscured. We converted the totally obscured reports to 8 (overcast) and partially obscured to 4 (four-eighths).

2.2.3 METAR Code. METAR code is the most difficult to work with in computing the total cloud-cover distribution. This is due to the fact there is no provision in the code for reporting the total cloud-cover. Cloud cover is reported only in layers, but these layered amounts are not cumulative as in the Airways code. The observer reports the fraction of cloud (in eighths) that is observed in each layer. Merely adding the layer coverage does not provide the total cloud cover, since the observer may report overlapping layers. An algorithm has been developed by USAFETAC to process these layered amounts to obtain a total cloud-cover; it is described in the Appendix. Values of partial and total obscuration are processed the same as with the synoptic code.

2.3 RTNEPH Total Cloud Cover. The RTNEPH total cloud cover is recorded to the nearest whole percent. There are two primary sources of these reports: surface observations and satellite analyses. If a nearby surface observation is available for the RTNEPH point of interest, this observation is used with no additional processing. The corresponding percentages for the Airways code categories of clear, scattered, broken, and overcast are 0%, 25%, 85%, and 100%. Reports for the synoptic code are converted to the corresponding percentage. RTNEPH uses an algorithm to determine the total cloud cover from METAR reports. If no surface observations are available, then a satellite analysis is used and reported in whole percent (for details, see Kiess and Cox, 1988). The RTNEPH-based total cloud cover distribution will then be a mix of these procedures. There is a flag in the RTNEPH database indicating the source of the total cloud cover reports. Separate frequency distributions should then be computed for surface- and satellite-based reports. While the type of surface report is not included, it is fairly easy to tell from examination of the frequency distribution if the surface observations are primarily Airways (large number of counts at 0%, 25%, 85%, and 100% total cloud-cover), or METAR/synoptic (counts at 0. 12%, 25%, 38%, etc.)

2.4 Burger Aerial Algorithm. Because of the discrete nature of surface cloud-cover reports, we make use of the Burger Aerial Algorithm (BAA) to convert the observed distribution to one with higher fidelity. The BAA (Burger, 1985) is actually a continuous distribution of cloud-cover, but for practical reasons, we use it to determine the probability of each of the cloud-cover frequency intervals listed in Table 2. (For a comprehensive review of this algorithm and a discussion of its accuracy, see Henderson-Sellers and McGuffie, 1991). The computational details of converting the Airways, METAR, or synoptic code to these intervals using the BAA are described in the Appendix. The categories in Table 2 are used to compute the climatological probability of CFLOS, as described in the next chapter.

TABLE 2. Cloud-cover intervals used for CPCFLOS calculations.

Category Number	Range (%)
1	0% - 5%
2	6% - 15%
3	16% - 25%
4	26% - 35%
5	36% - 45%
6	46% - 55%
7	56% - 65%
8	66% - 75%
9	76% - 85%
10	86% - 95%
11	96% - 100%

3. CALCULATION OF THE CLOUD-FREE LINE-OF-SIGHT PROBABILITIES

3.1 SRI Model. Lund and Shanklin (1973) developed a technique for relating fractional sky-cover to the climatological probability of cloud-free line-of-sight. This technique was derived from a collection of whole sky photos (Lund and Grantham, 1980) taken at Columbia MO. Marick et al. (1979) identified shortcomings of the Lund and Shanklin model and proposed a revised model that is partly derived from relationships in the cloud viewing geometry. This revised model is referred to as the Stanford Research Institute (SRI) model. Malick et al. (1979) describes this model in detail. In the SRI model, the probability of a cloud-free line-of-sight when looking straight up, P_n, is given by:

$$P_n(S) = 1 - \frac{S(1 + 3S)}{4} \tag{1}$$

where S is the fractional sky-cover as *viewed from the ground.* For other viewing angles, the following approach is used. First we define the **zenith** angle, θ, as the angle the desired line-of-sight makes with the vertical. The climatological probability of CFLOS, $P(\theta,S)$, given a zenith angle of θ and a fractional sky-cover S, is obtained using:

$$P(\theta,S) = P_N(S)^{(1 + b\tan\theta)} \tag{2}$$

where b is the average height-to-width ratio of clouds and is assumed to follow the relation:

$$b = 0.55 - \frac{S}{2} \tag{3}$$

To obtain the climatological probability of CFLOS for viewing angle θ [$P_c(\theta)$] the CFLOS probability for a given sky-cover value S [$P(\theta,S)$] is weighted by the relative frequency, $f(S)$, of the sky-cover value:

$$P_c(\theta) = \int_0^1 f(s)P(\theta,S)dS \tag{4}$$

In practice, a finite approximation to Equation 4 is used:

$$P_c(\theta) = \sum_{i=1}^{11} f_i P_i(\theta) \tag{5}$$

where f_i is the relative frequency of cloud-cover interval i and $P_i(\theta)$ is the corresponding CFLOS probability for this interval. The intervals typically used are shown in Table 2.

A comparison between observed cloud-free line-of-sight from GOES imagery with computed values from the SRI model are shown in Figure 1. The results show very good agreement. Warren (1991*b*) also presents a favorable comparison between predicted (using the SRI model) and observed climatological probabilities of sunny line-of-sight in Hawaii.

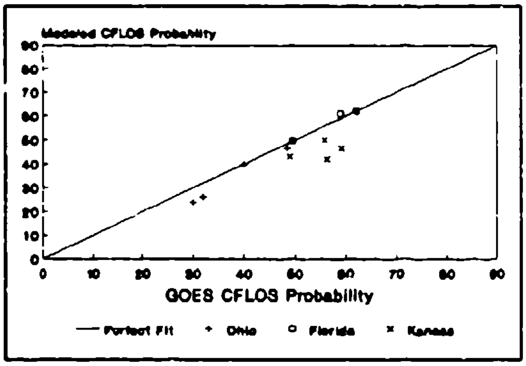

Figure 2. Comparison between predicted CPCFLOS values (from the SRI model) and values derived from GOES imagery at three locations (Results courtesy of Al Boehm, Hughes STX Corporation).

3.2 Space-Based Observations of Clouds. The SRI model assumes the fractional cloud-cover is determined by a surface observer. For locations with no surface observations available, cloud climatologies must be derived from satellite-based instruments. Such an approach is used by the USAF Real Time Nephanalysis (RTNEPH). However, surface and satellite observations of cloud-cover are distinct phenomena (Snow, 1990). Surface-based observations of fractional cloud-cover are often referred to as "sky-cover," while space-based observations are referred to as "earth-cover." The use of the SRI model with a cloud climatology derived from satellite data may produce significant errors. (A recent unpublished USAFETAC/SYT study found errors as high as 26%, with typical errors of 10-15%).

If we assume that the space-based observation is obtained by looking straight down at the point, the corresponding earth-cover for a given value of sky-cover can be obtained from:

$$Q = 1 - P_n \qquad (6)$$

where Q is the fractional earth-cover, and P_n is the probability of a surface-based cloud-free line-of-sight for vertical viewing. Combining Equation 4 with Equation 2, the corresponding sky-cover, (S), for a given value of earth-cover, $(Q,)$ is:

$$S = \left(\sqrt{\frac{4}{3}Q + \frac{1}{36}}\right) - \frac{1}{6} \qquad (7)$$

(**NOTE:** This equation is valid for *climatological* use only; in any given cloud scene, the relationship between S and Q must be defined in terms of a statistical distribution). For a given earth-cover, Q, using Equation 7 we can obtain the corresponding sky-cover, S, and then compute climatological CFLOS probabilities with Equations 1 through 3. Table 3 lists CFLOS probabilities for surface-based observations. Table 4 is the corresponding table for satellite-based cloud-cover.

3.3 Combining Sources. For RTNEPH-based calculations of CPCFLOS, two frequency distributions may be available for a point in question: one based on surface reports and one based on analyses of satellite observations. Separate CFLOS probabilities are obtained from each source. The final computed value is just a weighted average of the two sources:

$$\text{CPCFLOS} = \frac{N_1P_1 + N_2P_2}{P_1 + P_2} \qquad (8)$$

where P_1 and P_2 are the CPCFLOS probabilities determined from surface data and satellite data respectively, and N_1 and N_2 are the corresponding number of observations used for each computation.

TABLE 3. CFLOS probabilities as a function of viewing angle for each of the eleven cloud-coverintervals defined in Table 1. (*Surface*-based observations)

Deg	Cloud-Cover Category										
	1	2	3	4	5	6	7	8	9	10	11
0	0.99	0.97	0.92	0.86	0.78	0.69	0.58	0.46	0.32	0.17	0.04
10	0.99	0.96	0.91	0.85	0.77	0.67	0.57	0.45	0.31	0.16	0.04
20	0.99	0.96	0.91	0.84	0.76	0.66	0.55	0.43	0.30	0.16	0.04
30	0.99	0.96	0.90	0.83	0.74	0.64	0.54	0.42	0.29	0.15	0.04
40	0.99	0.95	0.89	0.81	0.73	0.63	0.52	0.40	0.28	0.14	0.04
50	0.99	0.95	0.88	0.80	0.70	0.60	0.49	0.38	0.26	0.14	0.03
60	0.99	0.94	0.86	0.77	0.67	0.57	0.46	0.35	0.24	0.12	0.03
70	0.98	0.92	0.83	0.72	0.61	0.50	0.40	0.30	0.20	0.10	0.03
80	0.97	0.88	0.74	0.61	0.48	0.36	0.27	0.19	0.12	0.06	0.01

TABLE 4. CFLOS probabilities as a function of viewing angle for each of the eleven cloud-cover intervals defined in Table 1. (*Satellite*-based observations)

Deg	Cloud-Cover Category										
	1	2	3	4	5	6	7	8	9	10	11
0	0.98	0.90	0.80	0.70	0.60	0.50	0.40	0.30	0.20	0.10	0.02
10	0.97	0.89	0.79	0.69	0.59	0.49	0.39	0.29	0.19	0.10	0.02
20	0.97	0.89	0.78	0.67	0.57	0.47	0.38	0.28	0.19	0.10	0.02
30	0.97	0.88	0.76	0.66	0.56	0.46	0.36	0.27	0.18	0.09	0.02
40	0.96	0.87	0.75	0.64	0.54	0.44	0.35	0.26	0.17	0.09	0.02
50	0.96	0.85	0.73	0.61	0.51	0.42	0.33	0.24	0.16	0.08	0.02
60	0.95	0.83	0.70	0.58	0.48	0.39	0.30	0.22	0.15	0.07	0.02
70	0.94	0.79	0.64	0.52	0.42	0.33	0.26	0.19	0.12	0.06	0.01
80	0.90	0.69	0.51	0.38	0.28	0.21	0.16	0.14	0.07	0.04	0.01

4. PROBABILITY OF CFLOS DURATION

4.1 Keilson-Ross Procedure. The technique described in Chapter 3 provides the probability of CFLOS for an instant in time. For some systems, a CFLOS window for successful viewing may be required. A technique for estimating duration probabilities of meteorological conditions is described by Gringorten (1982) and summarized here. This technique is known as the "Keilson-Ross algorithm" (Ross, 1980). Hering (1989) used this approach for computing the climatological probability of CFLOS duration.

If the probability of an event depends solely upon the outcome of the preceding trial, the sequence of events is called a *Markov process*, after the Russian mathematician A.A. Markov (Frieden, 1983). Weather elements are often modeled as Markov processes. The Ornstein-Uhlenbeck (O-U) process is a class of Markov processes in which the correlation coefficient (ρ) over the time interval (Δt) between the equivalent normal deviates (ENDs) of the two endpoints ($\tilde{y}_t$, $\tilde{y}_{t+\Delta t}$):

$$\rho = \exp\left(-\frac{\Delta t}{\tau}\right) \tag{9}$$

where τ is a parameter known as the "relaxation time." Hering (1989; 1990) recommends a τ-value of 30 minutes to calculate the correlation of CLOUD/NO CLOUD as a function of time for a fixed point in the sky (ρ). (For a discussion of equivalent normal deviates, see section A.2 in the Appendix.)

Given the value of a weather element at time t with a corresponding END of $\tilde{y}_t$, an END at time $t + \Delta t$ can be obtained stochastically using (Whiton and Berecek, 1982):

$$\tilde{y} = \rho\tilde{y}_t + \eta\sqrt{1 - \rho^2} \tag{10}$$

where η is a random normal number.

The cumulative probability that a weather element x is less than or equal to a threshold value (x_T) is the same probability that its END ($\tilde{y}$) is less than or equal to the END of the threshold value ($\tilde{y}_T$). This probability can thus be obtained from integrating the normal distribution curve:

$$\begin{aligned} P(x \le x_T) &= P(\tilde{y} \le \tilde{y}_t) \\ &= \frac{1}{2\pi}\int_{-\infty}^{\tilde{y}_t} \exp\left(-\frac{\tilde{y}^2}{2}\right) d\tilde{y} \end{aligned} \tag{11}$$

We can use the notation $F_{\Delta t}(x_T)$ to represent the cumulative probability of a weather element having a value less than or equal to a threshold (x_T) throughout a time duration Δt. This probability corresponds to the probability that the END of the weather element will have a value less than or equal to $\tilde{y}_T$ (the END of x_T) for a relative time period Θ (this is a dimensionless value--for the O-U process this corresponds to $\Delta t/\tau$):

$$F_{\Delta t}(x_T) = F_\Theta(\tilde{y}_T) \tag{12}$$

Equations 10 and 11 can be combined to obtain a functional relationship for $F_\Theta(\tilde{y}_T)$. For the special case when $\tilde{y}_T = 0$ (i.e., the case when x_T is the median value):

$$F_\Theta(0) = \frac{1}{\pi}\sin^{-1}(e^{-\Theta}) \tag{13}$$

Unfortunately this simple result is limited only to the specific case when the threshold is the median value. An analytical expression for the general solution has not been found. A complete description of the mathematics involved in obtaining an iterative solution is described in Gringorten (1982). Ross (1980) fitted this solution to a series of polynomials obtained from the use of a cubic spline algorithm. Gringorten (1982) provides the FORTRAN code to implement this algorithm.

4.2 Example. Suppose at a given location and time, the climatological probability of CFLOS (at an instant in time) for a zenith angle of 40° is 49%. We can use the Keilson-Ross procedure to compute the probability of CFLOS for time periods of t minutes. To plot the CPCFLOS as a function of the time window, we can first compute the values at selected points, such as 1, 2, 5, 10, 20, 30, 45, and 60 minutes. The correlations obtained from the O-U assumption are listed in Table 5. Also in Table 5 are the probabilities of CFLOS for the specified duration obtained from the Keilson-Ross algorithm. A plot of the results is shown in Figure 3. Results of a validation study for this technique in CFLOS calculations are presented in Hering (1989; 1990). This assumption that cloud-free line-of-sight is assumed to be a Markov process is clearly the limitation of this technique. Other models have been suggested (McCabe, 1968; Boehm, 1992*b*).

TABLE 5. Correlation between ENDs of cloud/no cloud values (ρ) and corresponding CPCFLOS as function of time window.

Time	ρ	Probability
0	1.00	0.49
1	0.97	0.46
2	0.94	0.45
5	0.85	0.42
10	0.72	0.39
20	0.51	0.35
30	0.37	0.33
45	0.22	0.29
60	0.14	0.27

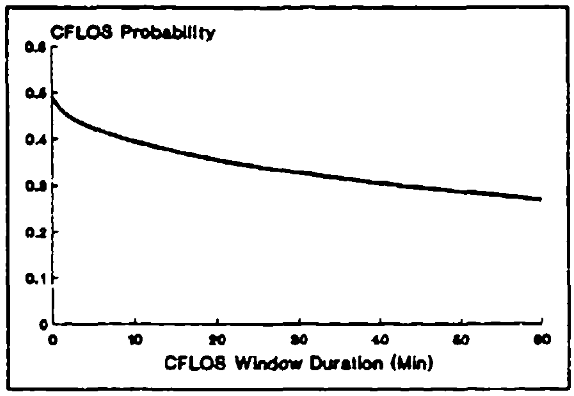

Figure 3. Climatological probability of cloud-free line-of-sight as a function of duration window.

5. SAMPLE CALCULATION

To illustrate how the climatological probability of CFLOS is obtained, consider the following example. Table 6 gives an example with two sample cloud-cover distributions. From this data, the parameters of the Burger Aerial Algorithm are computed using the method described in Appendix A. For this example, the mean sky cover values are 0.733 and 0.490, with sky dome scale distances of 6.551 km and 1.604 km for Points *A* and *B* respectively. The relative frequency distribution of cloud-cover, using the Burger intervals, are presented in Table 7. From this distribution, the climatological probability of CFLOS can be obtained using the data in Table 3. These results are presented in Table 8. The first column of results is for a CFLOS window of 0 (instantaneous probability), the second column is for a window of 10 min. These latter numbers were obtained by first using the Keilson-Ross algorithm to adjust the probabilities of CFLOS.

TABLE 6. Two sample cloud-cover frequency distributions.

Number of Observations		Relative Frequency
Point *A*		
CLR	346	0.208
SCT	101	0.061
BKN	98	0.058
OVC	1120	0.673
Point *B*		
CLR	414	0.263
SCT	376	0.248
BKN	412	0.258
OVC	364	0.231

TABLE 7. Relative cloud-cover frequency distribution for 11 cloud-cover categories.

Cloud-Cover	Relative Frequency	
	A	*B*
< 0.05	0.21	0.27
0.06 - 0.15	0.02	0.08
0.16 - 0.25	0.01	0.05
0.26 - 0.35	0.01	0.05
0.36 - 0.45	0.01	0.04
0.46 - 0.55	0.01	0.04
0.56 - 0.65	0.01	0.04
0.66 - 0.75	0.01	0.05
0.76 - 0.85	0.01	0.05
0.86 - 0.95	0.02	0.08
0.96 - 1.00	0.68	0.25

TABLE 8. Climatological Probability of CFLOS for each of the two sample datasets.

Zenith Angle	Instantaneous	10-minute Window
Point *A*		
0	31	26
10	31	26
20	30	26
30	30	25
40	29	25
50	29	25
60	29	24
70	28	24
80	26	22
Point *B*		
0	58	48
10	58	48
20	57	47
30	57	47
40	56	46
50	55	45
60	54	44
70	52	42
80	47	37

6. PROGRAM STRUCTURE

The techniques described in Chapters 3 and 4 are used by the USAFETAC CPCFLOS program. The program ingests cloud data from several possible sources (surface observations; the old 3-D nephanalysis, or 3DNEPH; and the real-tim‹ nephanalysis, or RTNEPH) and derives the climatological probability of cloud-free line-of-sight. A diagram of the program structure is depicted in Figure 4. The first row of subroutines shown in this figure lists the various readers used by CPCFLOS, depending on the type of data selected.

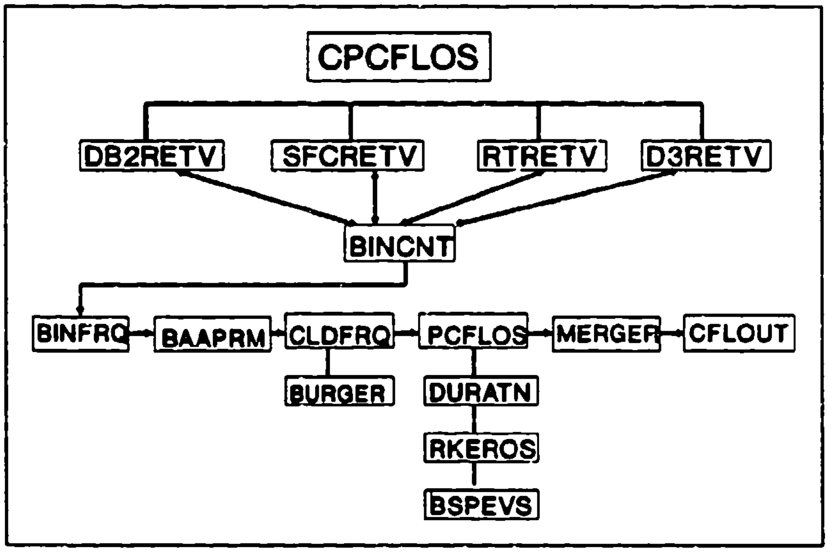

Figure 4. Structure of the computer program CPCFLOS.

CPCFLOS uses one of four readers to process sky-cover data. Subroutine DB2RETV retrieves data stored in DB2 tables (DB2 is the relational database management system on the USAFETAC mainframe. SFCRETV is used for DATSAV2 surface data (DATSAV2 is a USAFETAC-developed code format for archiving surface observations; for details see USAFETAC, 1986), RTRETV is used for RTNEPH data, and D3RETV for 3DNEPH, an earlier version of RTNEPH; for details see Coburn, 1970). After each observation is read in, the data is passed to subroutine BINCNT, which keeps track of the number of occurrences of each sky cover category, by month, and hour. RTNEPH data is also stratified by whether the cloud-cover was derived from a surface report or a satellite analysis.

The RTNEPH became operational on 1 June 1984. The drawback with 3DNEPH, its predecessor, is that no data source flag is available; users cannot be certain if an observation is surface- or satellite-based. CPCFLOS includes a flag, set by the user, to designate if there is a surface observing station within a 50-NM radius of the desired point. If such a station exists, CPCFLOS assumes that the 3DNEPH cloud-cover reports are surface-based; if not, it assumes they are satellite-based. Because of this serious limitation, the use of 3DNEPH to compute CFLOS probabilities should be avoided whenever possible.

Once all the observations have been read in, the subroutine BINFRQ is called. This routine computes the relative frequency of observed cloud-cover. Categories are in eighths of total cloud cover. (For Airways reports, clear skies are assigned a value of 0/8; scattered, 2/8; broken, 7/8; and overcast 8/8).

Next, control is passed to the subroutine BAAPRM, which computes the parameters of the Burger Aerial Algorithm. Two techniques are used: one for Airways data and one for data in eighths. An algorithm is used to examine the relative frequency distribution passed from BINFRQ. If the total number of observations in 2/8 exceeds the combined total in 1/8, 3/8, and 4/8, and if the total number in the category 7/8 exceeds the combined total in 5/8 and 6/8, the distribution is classified as Airways. This classification may occur with both surface- and NEPH-based data.

In the following step, the relative frequency distribution of cloud cover for the 11 intervals presented in Table 2 is computed by the subroutine CLDFRQ, which calls the subroutine "BURGER." When passed the mean sky cover, scale distance, and a value of cloud-cover, BURGER returns the probability of obtaining a cloud-cover less than or equal to the passed value.

Next, the subroutine PCFLOS computes the climatological probability of CFLOS given the relative frequency distribution computed by CLDFRQ. PCFLOS begins by computing the CFLOS probabilities for each cloud-cover interval and viewing angle, first for surface-based, then for satellite-based data. Next, if a time window other than zero is requested, each probability is passed to the function DURATN, which adjusts the probability for the time window using the Keilson-Ross procedure. This procedure is implemented by the subroutine RKEROS, which is an empirical fit to the analytical solution using cubic splines. The subroutine BSPERVS is needed to solve the cubic spline equations. PCFLOS returns separate CFLOS probability estimates: one for surface-based data, the other for satellite-based data.

The final routine to be called is MERGER, which combines the two CFLOS probabilities into one, using a weighted average. The individual probabilities are weighted by the number of observations used to derive it. This is the final value of CFLOS probability, which then appears on the output. The program output is created by subroutine CFLOUT.

APPENDIX

BURGER AERIAL ALGORITHM

A.1 Introduction. Surface observations of total cloud-cover are reported with low resolution. In the U.S., where most observations are recorded in the Airways code, cloud-cover is reported as either clear, scattered, broken, or overcast. Selected locations in the U.S. (and in most other countries as well) record an observation in synoptic code every 3 hours. In synoptic units are in *eighths* of total cloud-coverage. At most other locations throughout the world, the usual code for weather observations is METAR. Only layer amounts are encoded in METAR (in eighths); there is no report for total cloud-cover.

The limitations of using these codes to infer the distribution of cloud-cover is reviewed by Grantham and Boehm (1986). To overcome the low fidelity of the observations, Burger (1985) devised a model for specifying the cloud-cover distribution. We refer to this model as the *Burger Aerial Algorithm* (BAA). The model is a numerical fit to the results of multiple simulations, as described by Burger and Gringorten (1983). It converts the discrete observations present in all three codes to a continuous distribution. This algorithm was favorably reviewed by Henderson-Sellers and McGuffie (1991). Other, somewhat more complex, algorithms have been proposed (Boehm, 1992*a*).

The BAA has two fundamental variables: mean sky cover and sky-dome scale distance. Frequency distribution for various values of these variables are shown in Figure A-1, opposite. A large scale distance indicates cloud-cover distributions that are either predominantly clear or cloudy. In these instances, the mean is the least likely value to occur. A small scale distance, on the other hand, signifies a distribution centered about the mean.

A.2 Equivalent Normal Deviates. To understand the fundamentals of the Burger Aerial Algorithm, a basic understanding of transforming variables to a Gaussian domain (a process sometime referred to as *transnormalization*) is required. For details, see Boehm (1976) or Whiton and Berecek (1982). A normal deviate is a variable that follows a normal distribution with a mean of zero and a standard deviation of unity. A value of any other variable will have a one-to-one correspondence with this normal deviate through the cumulative frequency distribution. The corresponding value of the normal deviate (the one with the same cumulative probability as the value of the meteorological variable of interest) is referred to as its *equivalent normal deviate* (END). For example, assume the observed frequency of total cloud-cover of three-eighths or less at a given location is 35%. The corresponding value of the normal deviate with a cumulative probability of 35% is −0.385. In this case, the END of three-eighths cloud-cover is −0.385. This is an example of transforming to the Gaussian domain. The advantage of this transformation is that it permits the use of statistical operations, which require an assumption of normality. Most meteorological variables, especially the cloud-cover, are especially non-normal.

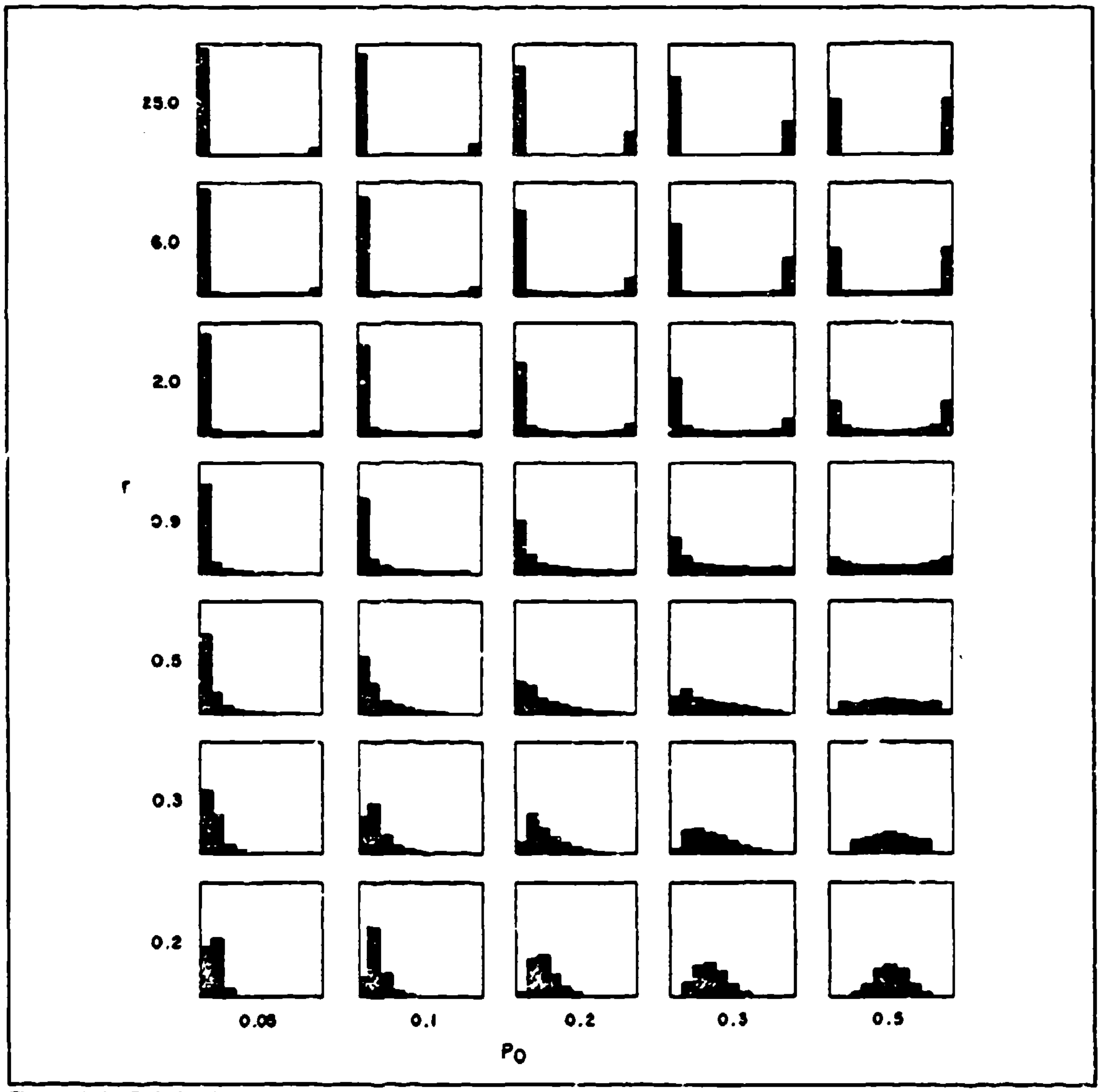

Figure A-1. Relative frequency distribution of cloud-cover for various values of the mean cloud-cover and sky dome scale distance (Burger, 1985).

A.3 Model Algorithm

A.3.1 Airways Code. Cloud-cover reports in Airways code are either clear, scattered, broken, or overcast. If we define the relative frequency of each category as CLR, SCT, BKN, and OVC, the BAA variables are computed as follows: First, the ENDs of CLR, SCT, and BKN are computed (Boehm, 1976) and referred to as y_{clr}, y_{sct}, and y_{bkn}. Differences between these values are then determined:

$$
\begin{aligned}
(\Delta y)_1 &= y_{bkn} - y_{clr} \\
(\Delta y)_2 &= y_{sct} - y_{clr} \qquad (14) \\
(\Delta y)_3 &= y_{bkn} - y_{sct}
\end{aligned}
$$

Next we consider three cases. Case 1 will be valid for most locations. Case 2, by exception, is when OVC is near zero. Case 3, also by exception, is when CLR is near zero. The scale distance parameter, (z), is computed using:

$$z = a + b\ln(\Delta y + c) \qquad (15)$$

where the particular value of Δy is determined from Equation (14) (For case 1, Δy_1, *etc.*). The coefficients a, b, and c for each case are listed in Table A-1. The END of mean cloud-cover is computed using:

$$y_0 = \frac{y}{1.9962 + 0.0022e^{-0.89z}} \qquad (16)$$

where y equals $0.5(y_{bkn} + y_{clr})$ for Case 1 and simply y_{bkn} for Cases 2 and 3. The sky-dome scale distance, (r), is then:

$$r = \frac{\sqrt{A}}{2^z} \qquad (17)$$

where A is the area of the sky dome, usually assumed to be 2424 km^2 (Burger, 1985).

TABLE A-1. Coefficients for computing the scale distance parameter, z.

Case	a	b	c
1	4.3580	1.7600	0.0670
2	5.5779	1.7600	0.0335
3	5.5779	1.7600	0.0335

A.3.2 Synoptic/METAR Code. Synoptic total cloud-cover reports are in eighths. METAR does not include a total cloud-cover report, but only individual layer amounts. The following algorithm developed at USAFETAC is used to compute the total fractional cloud-cover, (T), for N cloud-layers:

$$
\begin{aligned}
&T = X_1, \text{ for } N = 1 \\
&T = 0.85\sum_{i=1}^{N} X_i, \text{ for } N \geq 2 \qquad (18) \\
&\text{IF } T > 1 \text{ THEN } T = 1
\end{aligned}
$$

where X_i is the fractional cloud-cover for the ith layer.

The relative frequencies of each of the categories (0/8, 1/8, 2/8, ..., 8/8) are indicated by f_i where i ranges from 0 to 8 and indicates the eighths of coverage for that frequency interval. The ENDs of f_0, f_4, and f_7 coverage are computed (y_0, y_4, and y_7), then used to compute the following set of difference values:

$$
\begin{aligned}
(\Delta y)_1 &= y_7 - y_0 \\
(\Delta y)_2 &= y_4 - y_0 \qquad (19) \\
(\Delta y)_3 &= y_7 - y_4
\end{aligned}
$$

Two additional values (p_{40} and p_{74}) are computed: The value of the scale distance parameter z is computed using Equation 11 Equation 12 is used to compute the END of mean cloud-cover, (y_0).

$$p_{40} = f_4 - f_1$$
$$p_{74} = f_7 - f_4 \quad (20)$$

The coefficients used in this equation depend on one of the classes (4, 5, or 6). In most instances, Case 4 applies. Case 5 occurs when $f_8 < f_0$ and $f_8 < p_{74}$ and Case 6 occurs when $f_8 \geq f_0$ and $f_1 < p_{40}$. The value of y in eq. (4) is $0.5(y_7 + y_0)$ for Case 4 and y_4 for Cases 5 and 6.

TABLE A-2. Cloud-cover distribution used in the example.

Category	Rel Freq	Cum Freq	END
CLR	0.20	0.20	-0.8418
SCT	0.25	0.45	-0.1256
BKN	0.25	0.70	0.5244
OVC	0.30	1.00	∞

A.3.3 Example. To illustrate how these variables are computed, consider the following example. We will assume a location that uses Airways reporting has the following distribution of cloud-cover for the month and hour of interest: clear 20%, scattered 25%, broken 25%, and overcast 30%. The cumulative frequencies and their corresponding ENDs are shown in Table A-2.

This example follows Case 1. Computing the initial values:

$$(\Delta y) = y_{bkn} - y_{clr}$$
$$[0.5244 - (-0.8418)] = 1.3662 \quad (21)$$

$$Z = 4.3580 + [1.7600 \times \ln(1.3362 + 0.0670)]$$
$$= 4.8914 \quad (22)$$

$$y_0 = \{0.5(0.5244 - 0.8414)\} +$$
$$\{1.9962 + [0.0022 \times \exp(-0.89 \times 4.9914)]\}$$
$$= -0.0795 \quad (23)$$

This value is the END of the mean sky cover. This corresponds to a mean sky-cover of 0.53. To compute the scale distance:

$$r = \frac{\sqrt{2424}}{2^{4.9914}} = 1.55 \quad (24)$$

Thus, the Burger Distribution variables for the example in Table 10 are: mean sky cover 0.53, and scale distance 1.55 km.

A.4 Calculation of the Cumulative Frequency Distribution

A.4.1 Technique. Next, we present the technique for obtaining the continuous cumulative distribution of sky-cover, given the Burger distribution variables. To determine the probability, (P_x), of obtaining a fractional sky-cover of x or less, we compute F and t:

$$F = 10x, \quad x \leq 0.5$$
$$= 10(1 - x), \quad x > 0.5 \quad (25)$$

$$t = 1, \quad x \leq 0.5$$
$$= -1, \quad x > 0.5 \quad (26)$$

Recall that y_0 is the END of the mean sky-cover and z is the scale distance size. We then carry out the following calculations:

$$y_0' = t\, y_0 \quad (27)$$

$$N = 5 - \mathrm{INT}(F) \quad (28)$$

where INT(F) represents the integer portion of F [*e.g.*, INT(5.9) = 5]. The following additional calculations are made:

$$y_c = [0.9981 + 0.0011 \times \exp(0.89 \times z)] \times y_0' \tag{29}$$

IF N ≠ 0:

$$y_d = y_c + [A_N + B_N \times (C_N\, z)] \times (F + N - 6) \tag{30}$$

IF N > 1:

$$y_e = y_d - \sum_{i=1}^{N} [A_i - B_i \times \exp(C_i\, z)] \tag{31}$$

$$y_t = t\, y_e \tag{32}$$

This last value, (y_t), is the END of the desired probability P_x.

A.4.2 Example. Continuing with the example from the previous section (mean of 0.53 and scale distance of 1.55 km), what is the probability of a sky-cover of 30% or less (x = 0.30)?

$$F = 3 \quad y_0 = -0.0785$$
$$t = 1 \quad z = 4.9914$$
$$y_0' = -0.0795 \tag{33}$$
$$N = 2$$

$$y_c = (1.0916)(-0.0795) = -0.0868$$

$$y_d = -0.0868 + (-1) \times \{-0.0205 + [0.0097 \cdot (0.52 \cdot 4.9914)]\} = -0.1963 \tag{34}$$

$$y_e = -0.1963 + 0.0071 - [0.0086 \times \exp(0.53 \times 4.9914)] = -0.3104 \tag{35}$$

The END of the desired probability is -0.3104, which corresponds to a probability of 38%. Thus the probability of obtaining a total sky-cover of 30% or less is 38%, $P(x < 0.30) = 0.38$.

A.5 Calculations with the Normal Distribution. Since the integration of the normal probability density function has no known analytical solution, empirical approximations are used. These approximations are required in both transforming into and out of the Gaussian domain. The latter calculation is straightforward.

A.5.1 Converting an END to Its Probability. A fourth-order polynomial regression is used to provide an approximate solution to the integration of the normal probability density function. To determine the probability of obtaining an END of a value less than $\bar{y}$, $\Phi(\bar{y})$, the following algorithm is used (Abramowitz and Stegun, 1964):

$$\text{IF } \bar{y} \geq 0 \text{ THEN } T = 1 \qquad \text{IF } \bar{y} < 0 \text{ THEN } T = -1 \tag{36}$$

$$\Phi(\bar{y}) = \sum_{j=0}^{4} H_j\, (T\bar{y})^j \tag{37}$$

The coefficients H_j are listed in Table 11.

TABLE A-3. Coefficients used to convert from a probability to an END.

n	H_n
0	1.189
1	0.2341
2	0.1370
3	0.0004091
4	0.023221

A.5.2 Converting a Probability to Its END. Computing the END ($\tilde{y}$), from a probability (P) is more involved. The technique described here is from Beasley and Springer (1977). Simpler, but less accurate formulas are found in Boehm (1976). First we compute the parameter Q:

$$Q = P - 0.5 \tag{38}$$

If $|Q| \le 0.42$ use Equation 39:

$$\tilde{y} = \frac{\sum_{i=2}^{5} \alpha_{i-2} Q^{i}}{1 + \sum_{j=1}^{4} \beta_j Q^{j}} \tag{39}$$

The coefficients α_i and β_j are listed in Table A-4. For the case when $|Q| > 0.42$, first compute the parameter R:

$$\begin{aligned} &\text{IF } Q \ge 0 \text{ THEN:} \\ &\quad R = P \\ &\text{IF } Q < 0 \text{ THEN:} \\ &\quad R = 1 - P \end{aligned} \tag{40}$$

Next compute the parameter S:

$$S = [-\ln(R)]^{1/2} \tag{41}$$

The END $\tilde{y}$ is then:

$$\tilde{y} = T\left[\frac{\sum_{i=0}^{3} \gamma_i S^{i}}{1 + \sum_{j=1}^{2} \delta_j S^{j}}\right] \tag{42}$$

The coefficients γ_i and δ_j are listed in Table A-4.

TABLE A-4. Coefficients used to convert from a probability to its END.

n	α_n	β_n	γ_n	δ_n
0	2.5066	----	-2.7872	----
1	-18.6150	- 8.4735	-2.2980	3.5430
2	41.3912	23.0834	4.8501	1.6371
3	-25.4411	-21.0622	2.3212	----
4	----	3.1308	----	----

BIBLIOGRAPHY

Abramowitz, M. and I.A. Stegen, *Handbook of Mathematical Functions*, US Government Printing Office, Washington DC, 1964.

Beasely, J.D. and S.G. Springer, "The Percentage Points of the Normal Distribution," *Appl, Stat.*, Vol 26, *pp.* 118-121, 1977.

Boehm, A.R., "CUB: A General Purpose Coverage Algorithm," *Preprints of the Fifth International Meeting on Statistical Climatology*, American Meteorological Society, Boston MA, 1992*a*.

Boehm, A.R., "The Correlation of Waves in Time and Space," *Preprints of the 12th Conference on Probability and Statistics in Atmospheric Science*, American Meteorological Society, Boston MA, 1992*b*.

Burger, C.F., *World Atlas of Total Sky-Cover*, AFGL-TR-85-0198, Air Force Geophysics Laboratory, Hanscom AFB MA 01731, 1985.

Burger, C.F., and I.I. Gringorten, "Lineal and Areal Probabilities of Weather Conditions," *Preprints of the 8th Conference on Probability and Statistics in Atmospheric Science*, American Meteorological Society, Boston MA, 1983.

Cooper, A.R., *Three-Dimensional Nephanalysis*, AFGWC Technical Memorandum 70-9, Air Force Global Weather Central, Offutt AFB NE, 68113, 1970.

FMH-1, *Federal Meteorological Handbook No. 1: Surface Observations*, Office of the Federal Coordinator for Meteorological Services and Supporting Research, Washington DC, 1988.

Frieden, B.R., *Probability, Statistical Optics, and Data Testing*, Springer-Verlang, 1983.

Grantham, D.D., and A.R. Boehm, "The Effect of Viewing Aspect on Climatological Cloud Distortion," *Preprints of the Third International Conference on Statistical Climatology*, American Meteorological Society, Boston MA, 1986.

Gringorten, I.I., *The Keilson-Ross Procedure for Estimating Climatic Probabilities of Duration of Weather Conditions*, AFGL-TR-82-0116, Air Force Geophysics Laboratory, Hanscom AFB MA, 1982.

Gringorten, I.I. and A.R. Boehm, *The 3D-BSW Applied to Climatology of Small Areas and Lines*, AFGL/TR-87/0251, Air Force Geophysics Laboratory, Hanscom AFB MA, 1987.

Harms, D.E., *Cloud-Free Line-of-Sight (CFLOS) Simulation Models (Users Models)*, USAFETAC/PR-86/002, USAF Environmental Technical Applications Center, Scott AFB IL, 1986.

Henderson-Sellers, A. and K. McGuffie, "An Investigation of the Burger Distribution to Characterize Cloudiness," *J. Climate*, vol 4, *pp.* 1181-1209, 1991.

Hering, W.S., *Evaluation of Stochastic Models for Estimating the Persistence Probability of Cloud-Free Line-of-Sight*, GL-TR-89-0275, Geophysics Laboratory, Hanscom AFB MA, 1989.

Hering, W.S., *Probability Estimates of Cloud-Obscured Lin of-Sight*, GL-TR-90-0204, Geophysics Laboratory, Hanscom AFB MA, 1990.

Kiess, R.T., and W.M. Cox, *The AFGWC Automated Real-Time Cloud Analysis Model.* AFGWC/TN-88/001, Air Force Global Weather Central, Offutt AFB NE, 1988.

Lowther, R.P., M.T. Surmeier, R.W. Hartman, C.R. Coffin, and A.J. Warren, *RTNEPH Total Cloud Cover Validation Study*, USAFETAC/PR--91/020, USAF Environmental Technical Applications Center, Scott AFB IL, 1991.

Lund, I.A., and D.D. Grantham, "Estimating Probabilities of Cloud-Free Fields-of-View from the Earth through the Atmosphere," *J. Appl. Meteor.*, Vol 19, *pp.* 452-463, 1980.

Lund, I.A., and M.D. Shanklin, "Universal Methods for Estimating Probabilities of CFLOS through the Atmosphere," *J. Appl. Meteor.*, Vol 12, *pp.* 28-35, 1973.

Malick, J.D., J.A. Allen, and S. Zakanycz, "Universal Methods for Estimating Probabilities of CFLOS through the Atmosphere," *SPIE Vol 1 Atmospheric Effects on Radiative Transfer*, *pp.* 28-35, 1979.

McCabe, J.T., "Estimating Conditional Probabilities of Events Having Marked Diurnal Variability," *Preprints of the First National Conference on Statistical Meteorology*, American Meteorological Society, Boston MA, 1968.

Ross, H.F., *An Algorithm for $F_\theta(y)$ Using Cubic B-splines*, AFGL-TR-81-0068, Air Force Geophysics Laboratory, Hanscom AFB MA, 1980.

Rupp, J.A. and A.J. Warren, *The USAFETAC Cloud Scene Generator Model (CLDGEN)*, USAFETAC/TN--92/002, USAF Environmental Technical Applications Center, Scott AFB IL, 1992.

Snow, J.W., *Modeling the Variation of Cloud Cover with View Angle Using Space Shuttle Cloud Imagery*, GL-TR-90-0130, Geophysics Laboratory, Hanscom AFB MA, 01731-5000, 1990.

USAFETAC, *Climatic Database Users Handbook No. 4, DATSAV2 Surface*, USAFETAC/UH-86/004, Operating Location A, USAF Environmental Technical Applications Center, Asheville, NC, 1986.

Warren, A.J., *Optimum Placement of the Ground-Based Electrooptical Deep Space Surveillance (GEODSS) System*, USAFETAC/PR-91/018, USAF Environmental Technical Applications Center, 1991*a*.

Warren, A.J., *Simulated and Observed Sunny Line-of-Sight Probabilities at Palehua, Hawaii*, USAFETAC/PR-91/022, USAF Environmental Technical Applications Center, Scott AFB IL, 1991*b*.

Whiton, R.C., and E.M. Berecek, *Basic Techniques in Environmental Simulation*, USAFETAC/TN-82/004, USAF Environmental Technical Applications Center, Scott AFB IL, 1982.

ACRINABS

BAA	Burger aerial algorithm
BKN	broken (cloud-cover category)
CFLOS	cloud-free line-of-sight
CLR	clear (cloud-cover category)
CPCFLOS	climatological probability of cloud-free line-of-sight
OVC	overcast (cloud-cover category)
END	equivalent normal deviate
INT	integer function
O-U	Ornstein-Uhlenbeck
RTNEPH	real time nephanalysis
SCT	scattered (cloud-cover category)
SRI	Stanford Research Institute
SYT	Simulation and Techniques Branch
USAFETAC	United States Air Force Environmental Technical Applications Center
3DNEPH	3-dimensional nephanalysis

DISTRIBUTION

HQ USAF/XOOOW, Rm BD927, Washington, DC 20330-5054	1
OSAF/SS, Rm 4C1052, Pentagon, Attn: Weather, Washington, DC 20330-6560	1
USTC J3/J4-OW, Scott Dr., Bldg 1900, Scott AFB, IL 62225-7001	1
AWS/XTX/DO, Losey St., Bldg 1521, Scott AFB, IL 62225-5008	1
Det 3, DOXW, PO Box 95004, Henderson, NV 89009-5004	1
Det 4, AWS, Bldg 91027, Hurlburt Fld, FL 32544-5000	1
OL-B, HQ AWS, Hanscom AFB, MA 01731-5000	1
OL-K, HQ AWS, NEXRAD, 1200 Westheimer Dr., Norman, OK 73069-7902	1
OL-N, HQ AWS, ASL(SLCAS-BW-W), Bldg 1646, Rm 24, Missile Range, White Sands, NM 88002-5501	1
HQ AFGWC/DOM/SY, MBB39, 106 Peacekeeper Dr., Ste 2N3, Offutt AFB, NE 68113-4039	1
AFSFC/DON, Stop 82, Bldg 715, Patrick Ave., Falcon AFB, CO 80912-5000	1
USAFETAC, Scott AFB, IL 62225-5116	6
OL-A, USAFETAC, Federal Building, Rm 305, Asheville, NC 28801-2723	1
AFSPACECOM/DOWA, Bldg 1, Stop 7, Peterson Rd., Peterson AFB, CO 80914-5001	1
721SPTS Weather, STE 2-210, 1 Norad Rd, Cheyenne Mtn, CO 80914-6113	1
50 OSS/WE, Stop 82, Falcon AFB, CO 80912-5000	1
45WS, Bldg 423, C. St., Patrick AFB, FL 32925-6537	1
AFTAC/DOW, Patrick AFB, FL 32925-5000	1
30WS, Coral Rd., Bldg 21150, Vandenberg AFB, CA 93437-5000	1
SSD/MWA, PO Box 92966, Los Angeles, CA 90009-2960	1
SSD/IMO, PO Box 92960, Los Angeles, CA 90009-2960	1
SM-ALC/LH-AWS, McClellan AFB, CA 95652-5609	1
USAICS, Attn: ATSI-CDW, Ft Huachuca, AZ 85613-6000	1
CSTC/WE, 1080 Lockheed Way, Box 007, Bldg 1001, Sunnyvale, CA 94089-1230	1
OD 4/DX, Onizuka AFB, CA 94088-3430	1
SSD OD 4, Onizuka AFB, CA 94088-3430	1
Det 3, Space Systems, Bldg 430, Stop 77, Buckley ANGB, CO 80011-9599	1
AFMC(I)/DOW, Bldg 266, Post 108P Chidlaw Rd.,Wright-Patterson AFB, OH 45433-5000	1
FASTC/TAW, 4115 Hebble Creek Rd., Ste 33, Wright-Patterson AFB, OH 45433-5637	1
ASD/WE, Bldg 91, 3rd St, Wright-Patterson AFB, OH 45433-6503	1
AFIT/CIR, Wright-Patterson AFB, OH 45433-6583	1
WL/DOA, Wright-Patterson AFB, OH 45433-6543	1
WL/DOW, Wright Patterson AFB, OH 45433-6543	1
645 WS/CC, Wright-patterson AFB, OH 45433-5000	1
46 TG/WE, Holloman AFB, NM 88330-5000	1
PL/WE, Kirtland AFB, NM 87117-5000	1
HQ AFOTEC/WE, Kirtland AFB, NM 87117-7001	1
RL/WE, Griffiss AFB, NY 13441-5700	1
ROME LAB/SUL,Corridor W, Ste 262, 26 Electronic Pkwy, Griffiss AFB, NY 13441-4514	1
AFCESA/WE, Tyndall AFB, FL 32403-5000	1
AFESC/RDXT, Bldg 1120, Stop 21, Tyndall AFB, FL 32403-5000	1
ESD/WE, Vandenberg Dr., Bldg 1624, Hanscom AFB, MA 01731-5000	1
PL/TSML, Research Library, Hanscom AFB, MA 01731-5000	1
PL/GP, Hansom AFB, MA 01731-5000	1
3246TW/DOW, Bldg 60, Rm 60, Eglin AFB, FL 32542-5000	1
46 WS/CC, Eglin AFB,FL 31542-5000	1
AFFTC/WE, Edwards AFB, CA 93523-5000	1
SMC/SDW, PO Box 92960, Bldg 117, El Segundo, Los Angeles AFB, CA 90009-2960	1
UTTR/WE, Hill AFB, UT 84056-5000	1
USCENTCOM/CCJ3-W, Bldg 540, MacDill Blvd, MacDill AFB, FL 33608-7001	1
HQ AFTAC/TNK, 1030 Highway A1A, Patrick AFB, FL 32925-5000	1
ESMC/WE, Patrick AFB, FL 32925-5000	1
OL-A, AFCOS, Site R, Fort Ritchie, MD 21719-5010	1
USAFALCENT RA, Pope AFB, NC 28308-5000	1
CCSO/FL, Tinker AFB, OK 73145-6340	1
AFOSR/NL, Bolling AFB, DC 20332-5000	1
TFWC/WE, Nellis AFB, NV 89191-5000	1
SMC, Det 2/TDO, Onizuka AFB CA 94088-3430	1
AL/OEBE, 2402 East Drive, Brooks AFB, TX 78235-5114	1
AMC/XOWR, Bldg P40 N, Martin Ave, Scott AFB, IL 62225-5000	1

HQ AFSOC/DOW, Bldg 1, Hurlburt FLD, FL 32544-5000	1
ATC/DOTW, 244 F Street East, Suite #3, Randolph AFB, TX 78150-4325	1
Det 5, HQ AWS, Keesler AFB, MS 39534-5000	1
CFA, C-2/SWO, APO AP 96258-0210	1
PACAF/DOW, Bldg 1102, Hickam AFB, HI 96853-5000	1
Det 1, HQ PACAF, COMNAVMAR, PSC 489, Box 20, FPO AP 96540-0051	1
11WS, 1215 Flightline Ave, Ste 2, Eielson AFB, AK 99702-1520	1
USSTRATCOM/J3615, Rm L127, Bldg 522, 901 SAC Blvd, Offutt AFB, NE 68113-5000	1
2 WS/CC, Bldg 5546, 245 Davis Ave, Barksdale AFB, LA 71110-5002	1
ACC/DOW, Bldg 21, 30 Elm St, Ste 215, Langley AFB, VA 23655-2093	1
24WS, Unit 0640, APO AA 34001-5000	1
9COS/AOSW, Bldg 1130, Shaw Dr., Shaw AFB, SC 29152-5410	1
ATSI/CDW, US Army Intel, Ft Huachuca AI, AZ 85613-5000	1
USCENTCOM/CCJ3-W, MacDill AFB, FL 33608-7001	1
USSOCCENT/SCJ2-SWO, MacDill AFB, FL 33608-7001	1
USSOCOM/SOJ3-W, MacDill AFB, FL 33608-6001	1
1WG, Bldg 168, Hardee St., Ft McPherson, GA 30300-5000	1
USAFE/DOW, Unit 3050, Box 15, APO AE 09094-5000	1
17AF/DOW, Unit 4065, APO AE 09136-5000	1
HQ USEUCOM ECJ3, Unit 30400, Box 1000, APO AE 09128-4209	1
7WS, CINCUSAREUR/AREAWX, APO AE 09403-5000	1
16AF/SWO, Unit 6365, APO AE 09641-5000	1
COMNAVOCEANCOM, Code N312, Stennis Space Ctr, MS 39529-5000	2
COMNAVOCEANCOM (Capt Brown, Code N332), Stennis Space Ctr, MS 39529-5001	1
NAVOCEANO (Rusty Russum), Bldg 8100, Rm 203D, Stennis Space Ctr, MS 39522-5001	2
NAVOCEANO, Code 9220 (Tony Ortolano), Stennis Space Ctr, MS 39529-5001	1
Maury Oceanographic Library, Naval Oceanography Office, Stennis Space Ctr, MS 39522-5001	1
Naval Research Laboratory, Monterey, CA 93943-5006	1
Naval Research Laboratory, Code 4323, Washington, DC 20375	1
Naval Research Laboratory (Dr Riley), Code 4180, Washington, DC 20375 (SESS reports)	1
Naval Postgraduate School, Chmn, Dept of Meteorology, Code 63, Monterey, CA 93943-5000	1
Commanding Officer, Naval Polar Oceanography Center, 4301 Suitland Road, FOB #4, Washington, DC 20395-5108	1
Naval Oceanography Command Ctr, COMNAVMAR Box 12, FPO San Francisco, CA 96630-5000	1
Commanding Officer, Naval Oceanography Command Ctr, PSC 819, Box 13, FPO AE, 09645-3200	1
Chief, APG Met Team, Bldg 1134, Attn: AMSTE-TC-AM CAB, Aberdeen Proving Ground, MD 21005-5001	1
Atmospheric Sciences Laboratory (SLCAS-AS-I 3 10-2c), White Sands Missile Range, NM 88002-5501	1
TECOM Atmos Sci Div, AMSTE-TC-AA (MacBlain), White Sands Missile Range, NM 88002-5504	1
White Sands Met Team, AMSTE-TC-AM (WS), White Sands Missile Range, NM 88002-5501	1
USA TECOM, ATTN: AMSTE-TC-AM (RE) TECOM Met Team, Redstone Arsenal, AL 35898-8052	1
Director, U.S.A.-CETEC, Attn: GL-AE (Whitmarsh), Fort Belvoir, VA 22060-5546	1
Technical Library, Dugway Proving Ground, Dugway, UT 84022-5000	1
HQ NATO Staff Meteorological Officer IMS/OPS APO AE 09724	1
NOAA/MASC Library MC5, 325 Broadway, Boulder, CO 80303-3328	2
NOAA Library-EOC4W5C4, Attn: ACQ, 6009 Executive Blvd, Rockville, MD 20852	1
NOAA/NESDIS (Attn: Nancy Everson, E/RA22), World Weather Bldg, Rm 703, Washington, DC 20233	1
NGDC, NOAA, Mail Code E/GC4, 325 Broadway, Boulder, CO 80333-3328	1
NWS W/OSD, Bldg SSM C-2 East-West Hwy, Silver Spring, MD 20910	1
NIST Pubs Production, Rm A635, Admin Bldg, Gaithersburg, MD 20899	1
NASA-MSFC-ES44, Attn: Dale Johnson, Huntsville, AL 35812-5000	1
NASA-MSFC-ES44, Attn: Gwenevere Jasper, Huntsville, AL 35812-5000	1
DTIC-FDAC, Cameron Station, Alexandria, VA 22304-6145	2
AUL/LSE, Maxwell AFB, AL 36112-5564	1
AWSTL, Scott AFB, IL 62225-5438	35

END

FILMED

DATE: 2-93

DTIC